

Processing of Fluorescence Lifetime Image Using Modified Phasor Approach: Homo-FRET from the Acceptor

Yanzhou Zhou · Yulei Bai · Ci Chen · John M. Dickenson

Received: 11 September 2012 / Accepted: 24 February 2013 / Published online: 15 March 2013
© Springer Science+Business Media New York 2013

Abstract As the hardware of FLIM technique becomes mature, the most important criterion for FLIM application is the correct interpretation of its data. In this research, first of all, a more orthogonal phasor approach, called as Modified Phasor Approach (MPA), is put forward. It is a way to calculate the lifetime of the complex fluorescent process, and a rule to measure how much the fluorescence process deviates from single exponential decay. Secondly, MPA is used to analysis the time-resolved fluorescence processes of the transfected CHO-K1 Cell lines expressing adenosine receptor A₁R tagged by CYP and YFP, measured in the channel of the acceptor. The image of the fluorescence lifetime and the multiplication of the fluorescence lifetime and deviation from single exponential decay reveal the details of the Homo-FRET. In one word, MPA provides the physical meaning in its whole modified phasor space, and broadens the way for the application of the fluorescence lifetime imaging.

Keywords Phasor approach · Fluorescence lifetime · Homo-FRET

Introduction

Fluorescence is an important technique for investigating a variety of biological phenomena. Fluorescence lifetime (FLIM) is an intuitive parameter associated with fluorescence process [1], particularly, FERT: Fluorescence Resonance

Energy Transfer. The usual way to quantify FRET is to measure the shortening of the donor's lifetime, because the donor is quenched as FRET occurs [1]; however, accurate measurement of the donor's lifetime is difficult in some biological research, such as Homo-FRET. In fact, compared with the donor, the acceptor in the Homo-FRET is usually brighter than the acceptor/donor itself alone, and its average lifetime is also longer, which hints that this phenomenon can be used in the analysis of FRET. Some reports tried to use the acceptor's lifetime in the FRET to quantify the energy transfer efficiency; however, the hypothesis hasn't been verified by experiment.

In the scientific and engineering research, a physical phenomenon is often described by the orthogonal and linear transformation that preserves the lengths of the basic vectors and the basic angles between the vectors, in which every basic vector is independent from the others [2]. However, as linear models do not capture the rich dynamic behavior of the real world, non-orthogonal transformations are often used to unmix physical signals. In 1984, Jameson et al. proposed a transform method, referred to as phasor approach, Jameson's phasor approach, polar plot or AB plot, which can represents the time-resolved fluorescence processes in the phasor space graphically [3]. Although the transformation is nonorthogonal, it has been proven to be a valuable tool for the analysis of the time-resolved fluorescence processes [3–11]. The basic idea of Jameson's phasor approach is that a series of the time-resolved fluorescence images are transformed to a new phasor space, where different points represent the different fluorescence processes. This approach has distinct advantages, such as: i) immunizing to the light intensity interference; ii) simplifying FLIM analysis, by avoiding global fitting data; iii) allowing full quantization of the imaging of the specific fluorescence process, according to the trajectories of the selected data, which make the visual analysis of the different photophysical processes accessible to the nonprofessional [10]. However, its disadvantages are fatal,

Y. Zhou (✉) · Y. Bai · C. Chen
Faculty of Automation, Guangdong University of Technology,
Guangzhou, Guangdong 510006, People's Republic of China
e-mail: zhouyanzhou.optics@gmail.com

J. M. Dickenson
School of Science and Technology, Nottingham Trent University,
Nottingham NG11 8NS, UK

such as: i) its two unit vectors nonorthogonally depends on each other. Any change in one vector produces a change in the other one. ii) Jameson phasor space lacking in the physical meaning. Strictly, only the points on the universal circle represent single exponential decays, and any point deviating from the universal circle loses its physical meaning immediately. In order to bypass this mathematical embarrassment and retrieve physical meaning, researchers began to use “their own approach”, such as $(\tau_{\Delta\phi} + \tau_m)/2$, where $\tau_{\Delta\phi, m}$ are the fluorescence lifetime calculated from the modulation depth and phase shift, respectively, to estimate the average fluorescence lifetime for the complex fluorescence process [12].

Since the appearance of Jameson’s phasor approach at 1984, its mathematical basis has not been updated, although A. H. A. Clayton etc. has put forwards some inferences based on the linear interpolation, that allows to calculate the fluorescence lifetimes of two non-interactive components [5–7]. In the study, we first present a new theory called as Modified Phasor Approach (MPA) to interpret the time-resolved fluorescence process quantitatively; then introduce its application in the FRET; furthermore, simulate the time-resolved two-component fluorescence process; after describing the system setup, analyze the behaviors of CFP in the Homo-FRET, showing that the modified phasor approach is useful tool to characterize the FLIM imaging and analyze FRET in the cell biology.

Modified Phasor Approach (MPA) for the Analysis of the Time-Resolved Fluorescence Process

Modified Phasor Approach

When a pulse is used to excite a fluorescence sample, the fluorescence emission decays exponentially with time as

$$I(x, y, t) = \sum_{i=1}^q \alpha_i(x, y) \cdot \exp\left[-\frac{t}{\tau_i(x, y)}\right], \quad (1)$$

where τ_i and α_i are the corresponding fluorescence lifetime and intensity weighted fractional contribution of the i th fluorophores. The spatial coordinates (x, y) are omitted in the context below for simplicity. The Fourier transform of the fluorescence emission can be expressed

$$\tilde{I}(f) = \sum_{i=1}^q \frac{\alpha_i \cdot \tau_i}{\sqrt{1 + 4\pi^2 f^2 \tau_i^2}} \cdot \exp[-j \cdot \tan^{-1}(2\pi \cdot \tau_i \cdot f)], \quad (2)$$

where f is frequency. The modulation depth $m(f)$ and the phase shift between the excitation and the emission light $\Delta\phi(f)$ can be noted

$$m(f) = \frac{|\tilde{I}(f)|}{|\tilde{I}(0)|}, \quad \Delta\phi(f) = -\tan^{-1} \left\{ \frac{\text{Im}[\tilde{I}(f)]}{\text{Re}[\tilde{I}(f)]} \right\}, \quad (3)$$

where the symbols $|\cdot|$, $\text{Re}(\cdot)$ and $\text{Im}(\cdot)$ represent the amplitude, the real part and imaginary part of $\tilde{I}(f)$ or $\tilde{I}(0)$ -DC, respectively. If (2) and (3) are evaluated at a specific frequency f_0 , the measurement of the fluorescence lifetime image in the time domain or in the frequency domain should be equivalent. In the content below, f_0 is omitted from the expression of the function variables for convenience.

According to (3), $I(t)$ can be mapped to a phasor space (B, A) [3–11]

$$B = m \cdot \cos \Delta\phi, \quad A = m \cdot \sin \Delta\phi. \quad (4)$$

The fluorescence lifetimes τ_m , $\tau_{\Delta\phi}$, deduced from the modulation depth and the phase shift, respectively, can be described

$$\tau_m = (2\pi \cdot f_0)^{-1} \cdot \sqrt{\frac{1}{m^2} - 1}, \quad \tau_{\Delta\phi} = (2\pi \cdot f_0)^{-1} \cdot \tan(\Delta\phi). \quad (5)$$

(4) and (5) give out the basic descriptions of Jameson’s phasor approach. As much as the single-component fluorescence processes are concerned, $\tau = \tau_{\Delta\phi} = \tau_m$; however, as much as the multiple-component fluorescence processes, which are involved in the most cases of the biophysical studies, are concerned, these mathematical expressions are only an intermediate mathematical tool without any physical meaning.

One way to improve of Jameson’s phasor approach is to move the origin of the phasor space from $(0, 0)$ to $(0.5, 0)$,

$$B_m = m \cdot \cos(\Delta\phi) - 0.5, \quad A_m = m \cdot \sin(\Delta\phi). \quad (6)$$

Furthermore, polar coordinates can be used to rewrite (6)

$$\rho = \sqrt{B_m^2 + A_m^2}, \quad \theta = \tan^{-1} \left(\frac{A_m}{B_m} \right), \quad (7)$$

where ρ is the radial distance from the origin, and θ is the counter clockwise angle from the B -axis. The polar coordinates (ρ, θ) form a new space, called as modified phasor space. Therefore, the fluorescence lifetime can be deduced directly from the angle θ , denoted as

$$\tau_\theta = (2\pi \cdot f_0)^{-1} \cdot \sqrt{\frac{1 - \cos \theta}{1 + \cos \theta}}. \quad (8)$$

The theorem of (6) to (8), called as Modified Phasor Approach (MPA), can be applied to any case of the time-resolved fluorescence process, such as single component, multiple components and FRET, etc.

If a single-component fluorescence process is concerned, (8) can be simplified as,

$$\rho = 0.5, \quad \theta = \cos^{-1} \left[\frac{1 - (2\pi \cdot f_0)^2 \cdot \tau^2}{1 + (2\pi \cdot f_0)^2 \cdot \tau^2} \right]. \quad (9)$$

All the single-component fluorescence processes lie on the universal circle centred at $\rho = 0$, with a radius of 0.5. Depending on the phasor angle θ only, they are insensitive to the radial coordinate ρ , for $d\rho/d\tau = 0$. Every point in the modified phasor space, except the origin $\rho = 0$, has the definition of the fluorescence lifetime deduced from θ ; in the meantime, ρ can be used to depict the degree of the fluorescence process deviating from single-component fluorescence process. Any point of $\rho \neq 0.5$ can be considered to be a mixture of the multiple-component processes, located inside or outside the universal circle by the linear interpolation or extrapolation of each components. The points (0.5, 0) and (0.5, π) can be used to represent the fluorescence processes with the lifetime zero and infinite, respectively. The origin (0, 0) is a mathematical singularity.

As much as the fluorescence process of two non-interactive components are concerned, it can be mapped to a point (ρ , θ) in a chord on the universal circle, which intersects the circle at point (0.5, θ_1) and (0.5, θ_2), representing the fluorescence processes τ_1 and τ_2 , respectively, shown in the Fig. 1(a). α_1 , α_2 and τ_1 , τ_2 meet the condition,

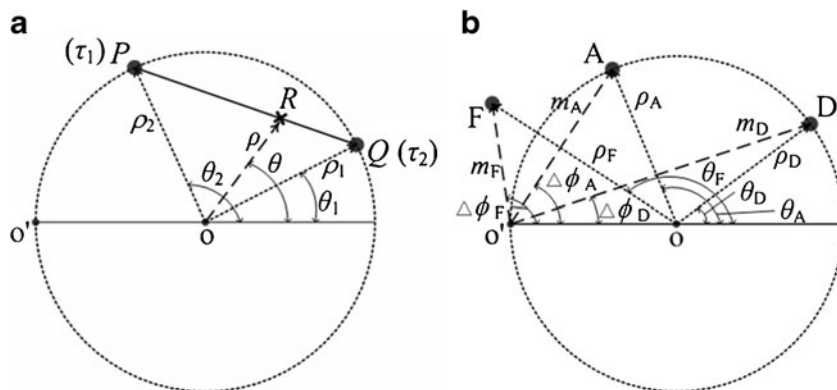
$$\frac{\alpha_1}{\alpha_2} = \frac{\sin(\theta_2 - \theta)}{\sin(\theta - \theta_1)} \cdot \frac{\tau_2}{\tau_1} \tag{10}$$

(10) shows that the ratio between the initial fluorescence intensities in the two-component fluorescence process is relative to their corresponding differences of the polar angles and the fluorescence lifetimes.

$$\rho_D = 0.5,$$

$$\theta_D = 2 \cdot \cos^{-1} \left\{ \left\{ \frac{\sin^2(\Delta\phi_F) + 2m_F \cdot \cos(\Delta\phi_F)}{2} + \frac{\sqrt{[\sin^2(\Delta\phi_F) + 2m_F \cdot \cos(\Delta\phi_F)]^2 - 4m_F^2}}{2} \right\}^{\frac{1}{2}} \right\} \tag{13}$$

Fig. 1 Modified Phasor Approach; **a** Modified Phasor Approach for FLIM, where P and Q represent single-exponent fluorescence processes and R represent two -component fluorescence process; **b** FRET process in the phase space and modified phase space, where F denotes FRET of the acceptor, A and D represent the donor in FRET and the acceptor free, respectively



FRET Analysis

FRET is a mechanism describing the energy transfer between the donor and acceptor molecules. As the fluorescence process of the FRET is measured in the acceptor channel using FLIM, the modulation depths m_F and the phase shift between the excitation and the emission light $\Delta\Phi_F$ of the FRET can be calculated, according to the (1) to (3); therefore, the coordinates (ρ_F , θ_F) of the FRET can be resolved, according to (6) to (7), shown in the Fig. 1(b).

The basic properties of the FRET in the Jameson phasor space are

$$m_F = m_D \cdot m_A, \quad \Delta\phi_F = \Delta\phi_D + \Delta\phi_A, \tag{11}$$

where m_D and m_A are the modulation depths of the donor in the FRET and the acceptor free, respectively; $\Delta\Phi_D$ and $\Delta\Phi_A$ are the phase shift between the excitation and the emission light of the donor in the FRET and the acceptor free, respectively. In the modified phasor space, (11) can be rewritten as

$$m_F = \cos\left(\frac{\theta_D}{2}\right) \cdot \cos\left(\frac{\theta_A}{2}\right), \quad \Delta\phi_F = \frac{1}{2}(\theta_D + \theta_A), \tag{12}$$

where (ρ_D , θ_D) and (ρ_A , θ_A) are the polar coordinates of the donor in the FRET and the acceptor free. Because (12) forms a group of the equations, its solutions are

and

$$\rho_A = 0.5,$$

$$\theta_A = 2 \cdot \cos^{-1} \left\{ \left\{ \frac{\sin^2(\Delta\phi_F) + 2m_F \cdot \cos(\Delta\phi_F)}{2} - \frac{\sqrt{[\sin^2(\Delta\phi_F) + 2m_F \cdot \cos(\Delta\phi_F)]^2 - 4m_F^2}}{2} \right\}^{\frac{1}{2}} \right\}, \quad (14)$$

where the definition domain of θ_D, θ_A is $[0, \pi]$.

Simulation

In order to verify the modified phasor approach, we take the time-resolved fluorescence process of two non-interactive components as an example,

$$I(t) = \sum_{i=1}^2 \frac{1}{\sigma_i \sqrt{2\pi}} \cdot \exp \left[-\frac{(\lambda - \mu_i)^2}{2\sigma_i^2} \right] \cdot \exp \left(-\frac{t}{\tau_i} \right), \quad (15)$$

where $\mu_1=470$ nm, $\sigma_1 = 20$ nm, $\tau_1=1$ ns, and $\mu_2=530$ nm, $\sigma_2 = 20$ nm, $\tau_2=20$ ns, respectively. The spectrum is shaped as a double peak Gaussian distribution, shown in the Fig. 2(a). At the frequency $f_0=60$ MHz, the modified phasor plot is shown in the Fig. 2(b), where the double-component fluorescence process is presented by a straight line intersected by the universal circle at the points denoting the single-component lifetimes $\tau_1=1$ ns and $\tau_2 =20$ ns, respectively, which is conformed to the report before [5]. Shown in the Fig. 2(c),

three wavelength-resolved lifetimes τ_θ, τ_m and τ_ϕ can be deduced, according to the modified phase approach and Jameson’s phase approach, respectively. τ_ϕ can be used to represent the single-component lifetime τ_1 at the wavelength ~ 470 nm; however, it is too ill-posed to tell another lifetime τ_2 . τ_m can properly stand for the single-component lifetime τ_2 at the wavelength ~ 530 nm, however, too ill-posed to tell the lifetime τ_1 . τ_θ switches rapidly between τ_1 at ~ 470 nm and τ_2 at ~ 530 nm. It can represent the two-component fluorescence process better than either $\tau_{\Delta\phi}$ or τ_m . The wavelength-resolved fluorescence parameters ρ, θ, m and $\Delta\phi$ are shown in the Fig. 2(d). m and $\Delta\phi$ response to the steady state from 470 nm to 530 nm by stepping up or down. In the meanwhile, the radius ρ responses to the transient state from 470 nm to 530 nm with a dip, and returns to the steady state $\rho =0.5$ which stands for the single-component fluorescence process.

System Setup

In order to verify the theory from (6) to (14), we built up a system based on the frequency domain lifetime method [13],

Fig. 2 Simulation of two non-interactive fluorophores and their parameters in the modified phasor space; **a** spectrum; **b** modified phasor plot; **c** τ_ϕ, τ_m and τ_θ ; **d** ρ, θ, m and $\Delta\phi$

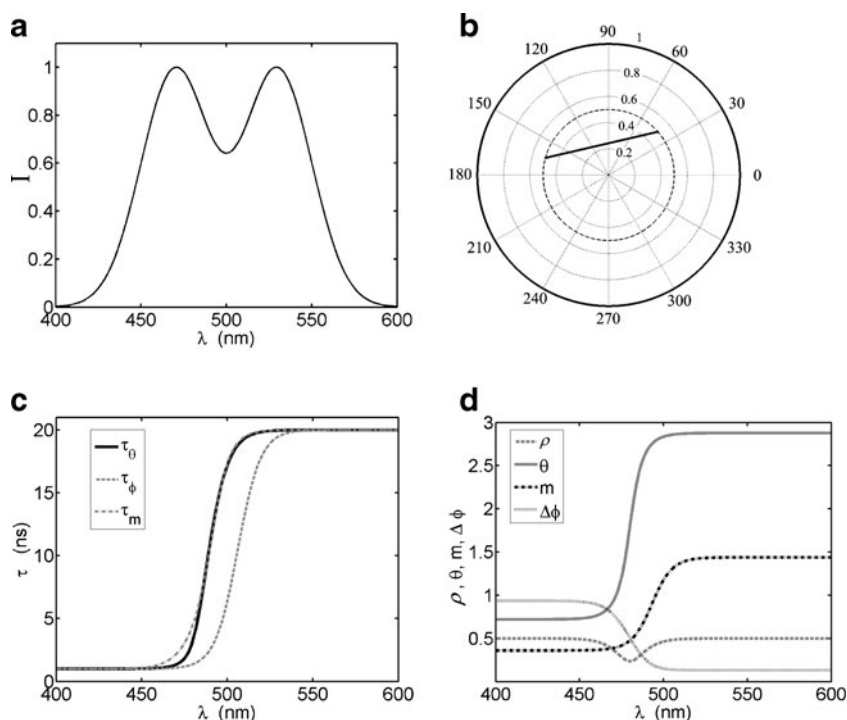
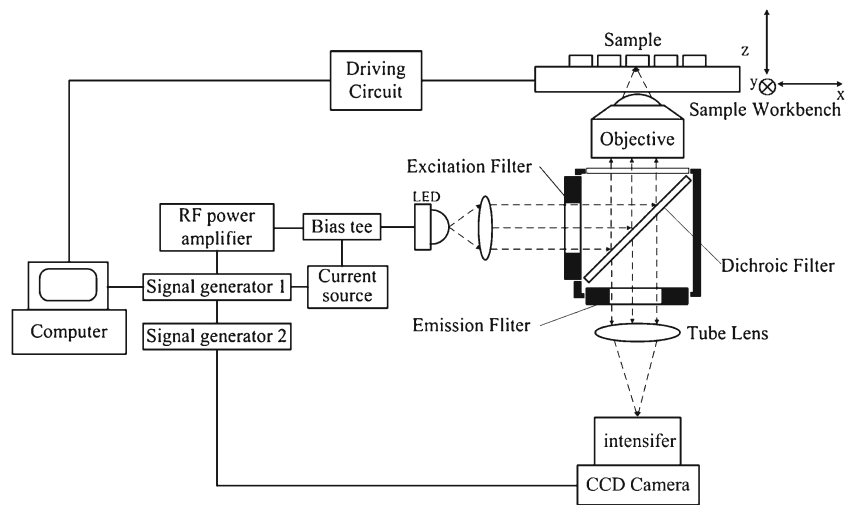


Fig. 3 FLIM system setup



shown in the Fig. 3. It was an add-on to a microscopy Olympus IX71, illuminated using a LUXEON III LED centered at 455 nm, with the spectral half width $\Delta\lambda_{1/2}=20$ nm (see Fig. 5(a)). The microscope was equipped with a filter set XF19-2 Vivid Plus (Excitation: 470DF35, Dichroic: 515DRLP, Emission: 515ALP, see Fig. 5(a)) and an Olympus LUCPlanFLN objective lens 40X NA=0.6. Emission light was directly mapped to an image intensifier modulated at 60 MHz and detected with a 14-bit cooled CCD camera. The LED and intensifier gain were modulated at the same frequency (60 MHz) signaled using two frequency generators which were phase locked between each other. A series of 16 images were acquired while the phase offsets between intensifier and LED was shifted at the step $\pi/8$ under the computer control. After Fourier transform, the modulation depth m and the phase shift $\Delta\phi$ between the

excitation and the emission light in the (3) can be recovered. In the end, the results from (6) to (14) can be obtained.

The standard sample was R6G solution prepared by deionized water with a final R6G concentration of 10 μ M. The biological sample was transfected CHO-K1 Cell lines expressing adenosine receptor A_1R tagged by CYP and YFP. CHO-K1 cells were grown in DMEM/F12 medium supplemented with 10 % fetal calf serum, 2 mM glutamine, penicillin streptomycin in a humidified atmosphere at 10 % CO_2 and at 37 $^\circ C$, using NUNC 96 glass plate. One of the cell images is shown in the Fig.4, after the fluorescence intensity is threshold over 1250.

Shown in the Fig. 5, the excitation efficiency of CFP is probably 8 times higher than YFP; in the meanwhile, the emission efficiency of YFP is 2 times higher than CFP. In the end, the emission efficiency of CFP is 4 times higher than YFP.

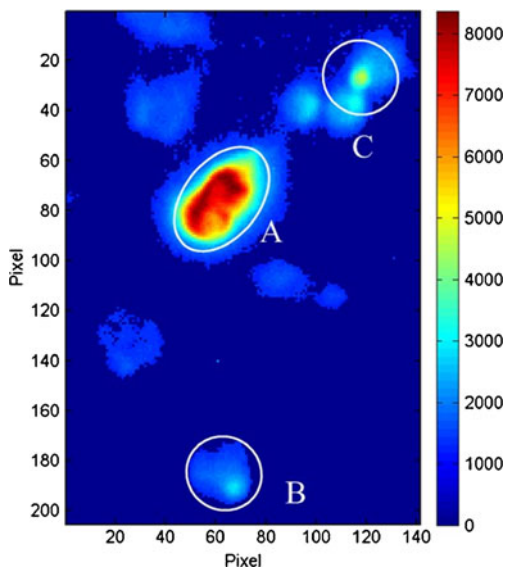


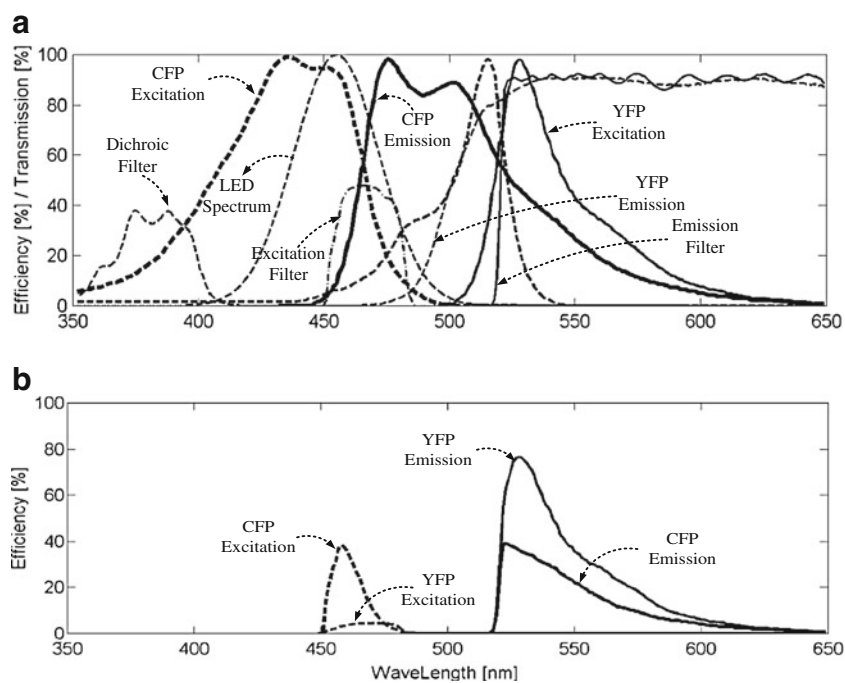
Fig. 4 Fluorescence image of the CHO-K1 cells expressing adenosine receptor A1R tagged by CYP and YFP, threshold over 1250

Experiment Results

Figure 6 shows the modified phasor histograms of 10 μ M rhodamine 6 G solutions. The modified phasor histogram of the fluorescence lifetime in the Fig. 6(a) is a Gaussian distribution with the centre located on the universal circle. Figure 6(b) shows that the peak of the histogram distribution of ρ is located at $\rho = 0.5$, which hints that the physics is a single-component fluorescence process. Figure 6(c) shows the peak of the histogram distribution of τ_θ is at 4.1 ns, which is conformed to the previous studies [13].

Figures 7 to 8 are the experimental results of the transfected CHO-K1 Cell lines expressing adenosine receptor A_1R tagged by CYP and YFP. First of all, all of the time-resolved fluorescence images of the cells are threshold between 650 and 1250. One of them is shown in the Fig. 7(a). Compared with the Fig. 4, it is easy to find that this is the image of the autofluorescence from the background. Its point-cloud map in the modified phasor space is shown in the Fig. 7(b) in the red,

Fig. 5 The Spectra of CFP, YFP, Filter set and LED; **a** the Spectra of CFP, YFP, Filter set and LED; **b** Excitation and emission efficiency of CFP and YFP



which is a typical Gaussian distribution with the center located at $(\rho, \theta) = (0.31, 139.6^\circ)$, representing the lifetime $\tau_\theta = 7.2$ ns. After the fluorescence intensity is threshold between 1250 to 1650, the point-cloud map in the modified phasor space is shown in the Fig. 7(b) in the blue, with the center located at $(\rho, \theta) = (0.36, 128.8^\circ)$, representing the lifetime $\tau_\theta = 5.5$ ns. With

the increasing the thresholding value, the center of the point-cloud moves upwards a bit, which is conformed to the report about the autofluorescence [10].

The fluorescence of the cell A in the Fig. 4 is from CFP in the Homo-FRET, due to: i) its fluorescence is brighter than others cells, for the excitation efficiency of CFP is

Fig. 6 Modified phasor histogram of the fluorescence lifetime of 10 μ M rhodamine 6 G solutions; **a** modified phasor histogram; **b** histogram of ρ ; **c** histogram of fluorescence lifetime τ_θ

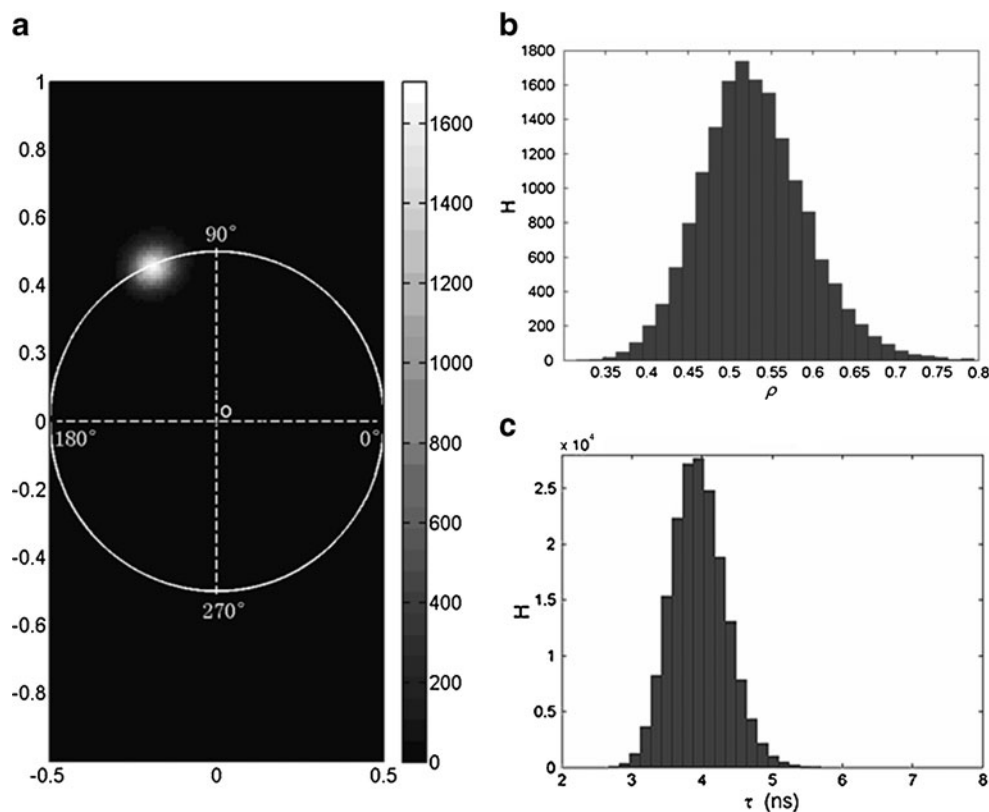
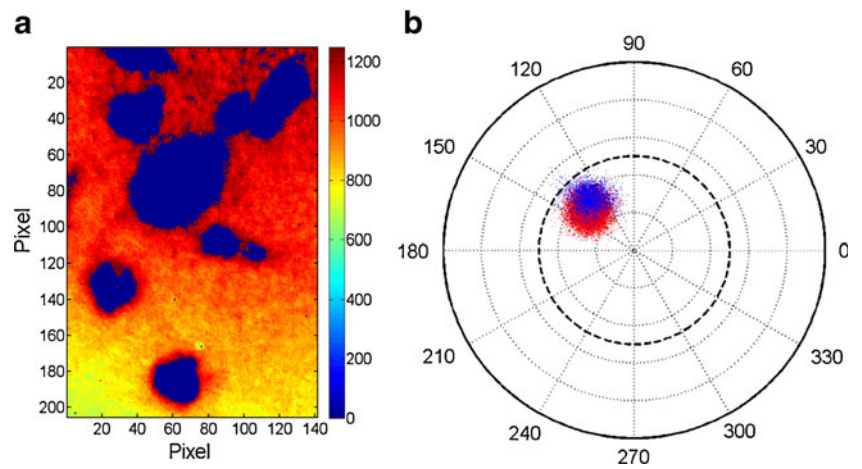


Fig. 7 Autofluorescence from the background; **a** image of the autofluorescence; **b** modified phasor plot



higher than that of YFP. ii) Homo-FRET happens. From the right to the left of the Fig. 8(a), the fluorescence lifetime become shorter and shorter; in the meanwhile, the fluorescence processing deviates more from single exponential decay shown in the Fig. 8(b). Figure 8(c) shows the multiplication of the fluorescence lifetime and the fluorescence process deviating from single exponential decay. The value in its outer ring to the left is low. These are the clues that the CFP is in the Homo-FRET. To be important, there is a place

at the cell A with high Homo-FRET energy-transfer efficiency, dark fluorescence (Fig. 8(d)), short lifetime, and deviation the most from the single exponential decay, marked in the Fig. 8. The fluorescence of CFP at the marked place is quenched deeply, in the meanwhile, the fluorescence proportion of the donor with a short lifetime increases shown in the Fig. 8(e). The distribution of the time-resolved fluorescence process of the cell A in the modified space is around the straight line in the red,

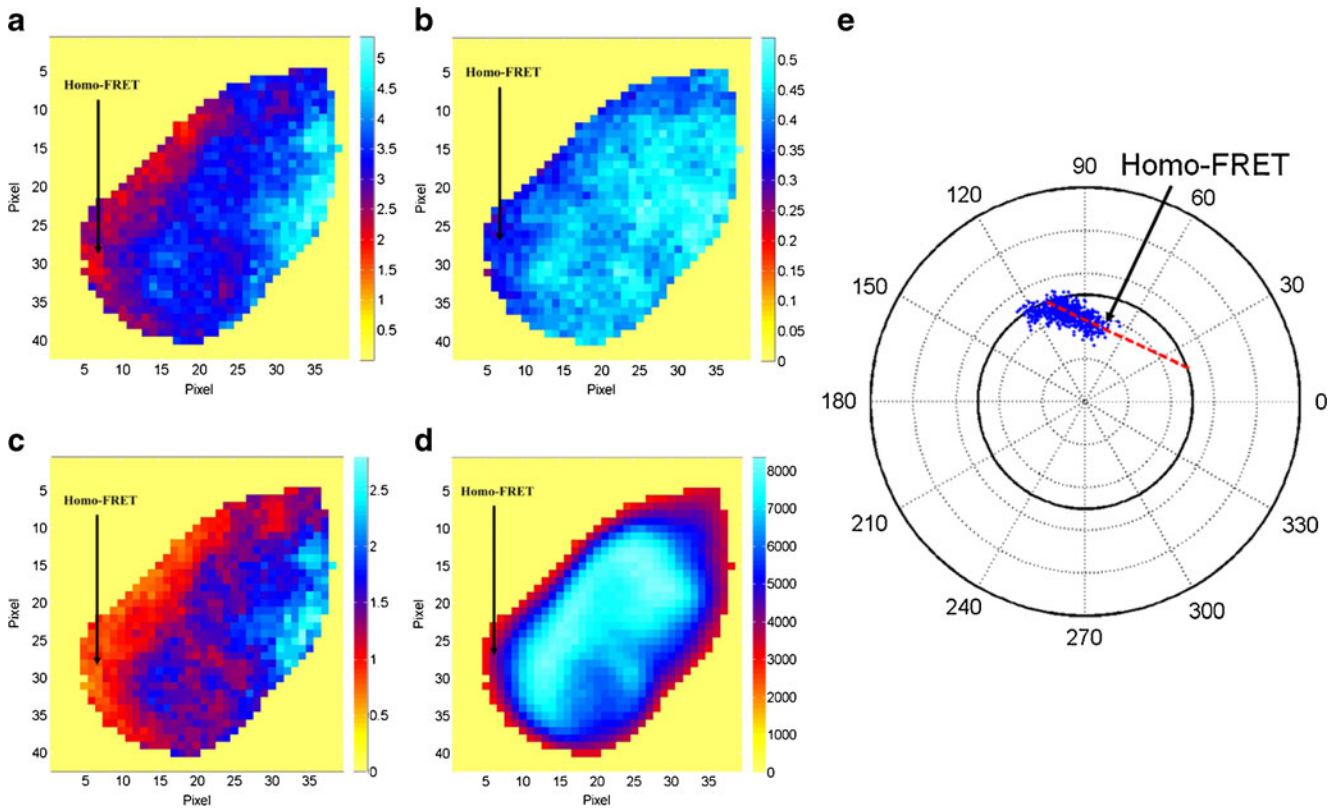


Fig. 8 Homo-FRET of CFP in the CHO-K1 cells expressing adenosine receptor A_1R tagged by CYP, after the fluorescence intensity was threshold over 3000; **a** image of the fluorescence lifetime; **b** image of the fluorescence deviation from single exponential decay ρ ; **c** image of

the multiplication between the fluorescence lifetime and the fluorescence deviation from single exponential decay $\rho \times \tau_0$; **d** image of the fluorescence intensity; **e** modified phasor plot

which is intersected with the universal circle at the points $(0.50, 111.4^\circ)$ and $(0.50, 18.4^\circ)$, respectively. In fact, the fluorescence from the cell A is composed of 3 components: CFP free, CFP as the donor and the acceptor in the Homo-FRET pair. Due to high FRET efficiency, The fluorescence of CFP free is too dim not to be distinguished in the modified phasor plot. This is a Homo-FRET distribution from the mixture of CFP as the donor and the acceptor. According to (8) and (11), the fluorescence lifetimes of CFP only, CFP as the donor and the acceptor in the Homo-FRET pair are $\tau_{\text{CFP}}=2.80$ ns, $\tau_{\text{D}}=0.43$ ns and $\tau_{\text{F}}=3.84$ ns, respectively. According to $E_{\text{FRET}}=(\tau_{\text{CFP}} - \tau_{\text{D}})/\tau_{\text{CFP}}$, the efficiency of the FRET is 84.6 %. $\tau_{\text{CFP}}=2.80$ ns is conformed to the fluorescence lifetime of CFP reported before [14].

Conclusions and Discussions

In this research, by moving the origin of the Jameson phasor coordinates to the new point $(0.5, 0)$, and adopting a polar coordinate, we put forwards a more orthogonal phasor approach, which provides a different metric for the explanation of the fluorescence process. One basic vector is the polar angle θ , which offers a way to calculate the fluorescence lifetime. Another basic vector is the radial coordinate ρ , which is a rule for measuring how much the fluorescence process deviates from single exponential decay. Compared to Jameson's phasor approach, this modified phasor approach defines a clear physics meaning of the fluorescence time in its whole modified phasor space, particularly for those fluorescence processes away from single exponential decay.

Although neither Jameson's phasor approach nor this modified one strictly adheres to the condition of the orthogonal transformation, the latter one is more orthogonal than the former one. It means that fluorescence lifetime deduced from the polar angle in the Modified Phasor Approach can reflect the intrinsic properties of fluorescence process better than Jameson's approach.

As the lifetime changes from $\tau=0$ to ∞ , $\Delta\phi$ in Jameson's phasor approach sweeps the range of $\pi/2$, while θ in the modified phasor approach sweeps the range of π , which

enlarges the dynamic range twice for evaluating the fluorescence lifetime. Furthermore, it can tolerate noise more, for $\rho/d\tau = 0$ at the universal circle.

Acknowledgment This work was partially supported by the Engineering and Physical Sciences Research Council, UK, under a Life Science Interface Grant EP/E013422/1, and is mainly supported by 211 Project, Guangdong province, P. R. China, under Grant YueFaGai 2009 [432]. The author is grateful to Dr. Q. S. Hanley at Nottingham Trent University, UK for his encouragement and helpful discussions.

References

1. Lakowicz JR (2006) Principles of fluorescence spectroscopy, 3rd edn. Springer, New York
2. Kreyszig E (2005) Advanced engineering mathematics. John Wiley & Sons, Orlando
3. Jameson DM, Gratton E, Hall RD (1984) The measurement and analysis of heterogeneous emissions by multifrequency phase and modulation fluorometry. *Appl Spectrosc Rev* 20:55–106
4. Jares-Erijman EA, Jovin TM (2003) FRET imaging. *Nat Biotechnol* 21:1387–1395
5. Clayton AHA, Hanley QS, Verveer PJ (2004) Graphical representation and multicomponent analysis of single-frequency fluorescence lifetime imaging microscopy data. *J Microsc* 213:1–5
6. Verveer PJ, Bastiaens PIH (2003) Evaluation of global analysis algorithms for single frequency fluorescence lifetime imaging microscopy data. *J Microsc* 209:1–7
7. Hanley QS, Clayton AHA (2005) AB-plot assisted determination of fluorophore mixtures in a fluorescence lifetime microscope using spectra or quenchers. *J Microsc* 218:62–67
8. Hanley QS (2009) Spectrally resolved fluorescent lifetime imaging. *J R Soc Interface* 6:S83–S92
9. Grecco HE, Roda-Navarro P, Verveer PJ (2009) Global analysis of time correlated single photon counting FRET-FLIM data. *Opt Express* 17:6493–6508
10. Digman MA, Caiolfa VR, Zamai M, Gratton E (2008) The phasor approach to fluorescence lifetime imaging analysis. *Biophys J* 94: L14–L16
11. Redford GI, Clegg RM (2005) Polar plot representation for frequency-domain analysis of fluorescence lifetimes. *J Fluoresc* 15:805–815
12. Leray A, Spriet C, Trinel D, Blossey R, Usson Y, Heliot L (2011) Quantitative comparison of polar approach versus fitting method in time domain FLIM image analysis. *Cytom Part A* 79A:149–158
13. Zhou Y, Dickenson JM, Hanley QS (2009) Imaging lifetime and anisotropy spectra in the frequency domain. *J Microsc* 234:80–88
14. Wouters FS, Esposito A (2008) Quantitative analysis of fluorescence lifetime imaging made easy. *J of HFSP* 2:7–11